PAPER

Precoded Physical Layer Network Coding with Coded Modulation in MIMO-OFDM Bi-Directional Wireless Relay Systems

Satoshi DENNO[†a)], ***Senior Member***, **Kazuma YAMAMOTO**[†], ***and*** **Yafei HOU**[†], ***Members***

SUMMARY This paper proposes coded modulation for physical layer network coding in multiple input multiple output orthogonal frequency division multiplexing (MIMO-OFDM) bi-directional wireless relay systems where precoding is applied. The proposed coded modulation enables the relays to decode the received signals, which improves the transmission performance. Soft input decoding for the proposed coded modulation is proposed. Furthermore, we propose two precoder weight optimization techniques, called "per subcarrier weight optimization" and "total weight optimization". This paper shows a precoder configuration based on the optimization with the lattice reduction or the sorted QR-decomposition. The performance of the proposed network coding is evaluated by computer simulation in a MIMO-OFDM two-hop wireless relay system with the 16 quadrature amplitude modulation (QAM) or the 256QAM. The proposed coded modulation attains a coding gain of about 2 dB at the BER of 10^{-4}. The total weight optimization achieves about 1 dB better BER performance than the other at the BER of 10^{-4}.

key words: *relaying, coded modulation, network coding, soft input decoding, non-linear precoding, quadrature amplitude modulations*

1. Introduction

Relaying has been used in wireless communication systems and is being considered for emerging wireless communication systems, because relaying potentially enables wireless systems to increase their coverage and improve the network capacity. Network coding has been investigated in wireless communication networks, because network coding further improves the transmission efficiency of bi-directional wireless relay systems. Especially, physical layer network coding (PLNC) has been considered in wireless bi-directional communication systems to increase the frequency utilization efficiency [1]–[3], which is one of the most important issues in wireless communication systems. Especially, exclusive-OR PLNC (XOR-PLNC) has been shown to achieve the upper bound in terms of channel capacity [4], [5]. XOR-PLNC has been extended for multiple input multiple output (MIMO) bi-directional relay channels, and its performance has been analyzed [6]–[8]. Because multiple radio signals are simultaneously received at relays when the PLNCs are applied, sophisticated receivers are needed on the relays [9]. Error correction coding has been introduced for performance enhancement [10]–[14]. Precoding [15] has been considered for the XOR-PLNCs for further performance enhancement [16]. Although the detection techniques to achieve the theoretical upper-bound have been shown [12]–[14], [16], those techniques are difficult to apply to relays due to prohibitive high computational complexity of the detectors. Reduced complexity detection in conjunction with unitary precoding has been proposed to achieve near optimum performance [17]. Non-linear precoding based on the Tomlinson Harashima precoding (THP) [18]–[21] has been proposed for the XOR PLNCs in MIMO bi-directional relay channels in order to achieve superior performance, while keeping the computational load on relays as small as possible [22]. Although most XOR-PLNC systems have been proposed for lower-order modulation schemes such as the binary phase shift keying (BPSK) and the quaternary phase shift keying (QPSK), the concept of them can be extended to quadrature amplitude modulations (QAMs) [22]. Even though the signal received at the relays can be decoded and forwarded when the BPSK or the QPSK is applied, the decoding has been impossible to apply at the relays when higher-order QAMs, e.g., the 16QAM, are used.

This paper proposes coded modulation for the PLNC with higher-order QAMs in MIMO orthogonal frequency division multiplexing (OFDM) bi-directional relay systems where precoding is employed. The proposed coded modulation enables the relays to decode the received signals, which improves the transmission performance. Soft input decoding for the proposed coded modulation is proposed. Furthermore, we propose two precoder weight optimization techniques, called as "per subcarrier weight optimization" and "total weight optimization". We show a precoder configuration based on the proposed optimization technique with the lattice reduction or the sorted QR-decomposition. The superior performance of the PLNC with the proposed techniques is confirmed in a MIMO-OFDM bi-directional relay system by computer simulation.

Next section describes a system model of a MIMO-OFDM bi-directional relay system, and our proposed techniques are explained in Sect. 3. The performance of the PLNC with the proposed technique is evaluated by computer simulations in Sect. 4. Finally, Sect. 5 concludes this paper.

Throughout the paper, $(\mathbf{A})^{-1}$, superscript T, and superscript H denote an inverse matrix of a matrix $\mathbf{A}$, transpose, and Hermitian transpose of a matrix or a vector, respectively. $\mathrm{tr}[\mathbf{A}]$ denotes trace of a diagonal matrix A. j indicates the imaginary unit. $\mathrm{E}[\zeta]$, $\Re[\alpha]$, and $\Im[\alpha]$ represent the ensemble average of a variable ζ, a real part, and an imaginary part of a complex number α.

Manuscript received March 24, 2020.
Manuscript revised June 5, 2020.
Manuscript publicized July 14, 2020.

[†]The authors are with Graduate school of natural science and technology, Okayama University, Okayama-shi, 700-8530 Japan.
a) E-mail: denno@okayama-u.ac.jp

DOI: 10.1587/transcom.2020EBP3045

2. System Model

We assume a wireless system where two terminals communicate with each other via relays. Those two terminals are called as "terminal A" and "terminal B", respectively, in this paper. While N_{T} antennas are placed on those terminals, only one antenna is employed in every relay. We assume that the N_{R} relays are placed between the two terminals. When the PLNC is applied to the communication between them, those terminals simultaneously transmit their own packets for the relays in the first slot, and the relays broadcast the packets for the two terminals in the second slot. As is described above, time division duplex (TDD) is applied for those terminals to exchange the information.

In the system, information bit streams are modulated with the proposed coded modulation that is explained below. Every modulation signal stream from the coded modulator is precoded with the proposed non-linear precoder that is also explained in the following section. All the precoder output modulation signal streams are provided to the inverse Fourier transform (IFFT) for generating OFDM signals. Let a variable Ω take A or B, the OFDM transmit signal vector $\mathbf{X}_{\Omega}(k) \in \mathbb{C}^{N_{\mathrm{T}}\times 1}$ from terminal Ω at time k can be written as,

$$\mathbf{X}_{\Omega}(k) = \frac{1}{\sqrt{N_{\mathrm{F}}}} \sum_{n=0}^{N_{\mathrm{F}}-1} \mathbf{X}_{\Omega,n} \mathrm{e}^{\mathrm{j}2\pi \frac{nk}{N_{\mathrm{F}}}}. \tag{1}$$

$\mathbf{X}_{\Omega,n} \in \mathbb{C}^{N_{\mathrm{T}}\times 1}$ and $N_{\mathrm{F}} \in \mathbb{N}$ in (1) denote the transmission signal vector on the nth subcarrier and the number of the IFFT points, respectively. As is described above, the transmission signal vector $\mathbf{X}_{\Omega,n}$ is precoded with the non-linear spatial filter as follows [23].

$$\mathbf{X}_{\Omega,n} = \mathbf{W}_{\Omega,n} \left(\mathbf{S}_{\Omega,n} + \mathbf{K}_{\Omega,n} L_{\mathrm{d}}\right) \tag{2}$$

In (2), $\mathbf{W}_{\Omega,n} \in \mathbb{C}^{N_{\mathrm{T}}\times N_{\mathrm{R}}}$, $\mathbf{S}_{\Omega,n} \in \mathbb{C}^{N_{\mathrm{R}}\times 1}$, $\mathbf{K}_{\Omega,n} \in \mathbb{C}^{N_{\mathrm{R}}\times 1}$ and $L_{\mathrm{d}} \in \mathbb{R}$ represent a precoding matrix, a modulation signal vector, a Gaussian integer vector on the nth subcarrier, and modulus for modulo operation on all the subcarriers[†], respectively. The two terminals simultaneously send their own packets containing those OFDM transmit signal vectors for the relays after the cyclic prefix is added, and those packets are received at every relay. Let $y_i(k) \in \mathbb{C}$ represent the kth received signal of the packets at the ith relay, all the signals received at the relays can be defined as $\mathbf{Y}_{\mathrm{R}}(k) = (y_1(k) \cdots y_{N_{\mathrm{R}}}(k))^{\mathrm{T}} \in \mathbb{C}^{N_{\mathrm{R}}\times 1}$ where $\mathbf{Y}_{\mathrm{R}}(k)$ denotes a received signal vector consisting of the signals received at the relays. The received signal vector $\mathbf{Y}_{\mathrm{R}}(k)$ can be written in the following equation[††].

$$\mathbf{Y}_{\mathrm{R}}(k) = \mathbf{H}_{\mathrm{A}}\mathbf{X}_{\mathrm{A}}(k) + \mathbf{H}_{\mathrm{B}}\mathbf{X}_{\mathrm{B}}(k) + \mathbf{N}(k) \tag{3}$$

[†]The modulo operation is employed in the non-linear precoding. The detail is explained in the following section.

[††]Although the cyclic prefix is actually added to the transmission signal vectors $\mathbf{X}_{\Omega}(k)$, the cyclic prefix is not written for simplifying the explanation and the mathematical expression.

$\mathbf{H}_{\mathrm{A}} \in \mathbb{C}^{N_{\mathrm{R}}\times N_{\mathrm{T}}}$, $\mathbf{H}_{\mathrm{B}} \in \mathbb{C}^{N_{\mathrm{R}}\times N_{\mathrm{T}}}$, and $\mathbf{N}(k) \in \mathbb{C}^{N_{\mathrm{R}}\times 1}$ in (3) denote a channel matrix between the relays and the terminal A, that between the relays and the terminal B, and the additive Gaussian noise (AWGN) vector, respectively. Let $\mathbf{Y}_{\mathrm{R},n} \in \mathbb{C}^{N_{\mathrm{R}}\times 1}$ represent the nth subcarrier signal vector received at the relays, the subcarrier signal vector can be expressed as,

$$\begin{aligned}\mathbf{Y}_{\mathrm{R},n} &= \frac{1}{\sqrt{N_{\mathrm{F}}}} \sum_{k=0}^{N_{\mathrm{F}}-1} \mathbf{Y}_{\mathrm{R}}(k) \mathrm{e}^{-\mathrm{j}2\pi \frac{nk}{N_{\mathrm{F}}}} \\ &= \mathbf{H}_{\mathrm{A},n}\mathbf{X}_{\mathrm{A},n} + \mathbf{H}_{\mathrm{B},n}\mathbf{X}_{\mathrm{B},n} + \mathbf{N}_{\mathrm{R},n}. \end{aligned} \tag{4}$$

In (4), $\mathbf{H}_{\mathrm{A},n} \in \mathbb{C}^{N_{\mathrm{R}}\times N_{\mathrm{T}}}$, $\mathbf{H}_{\mathrm{B},n} \in \mathbb{C}^{N_{\mathrm{R}}\times N_{\mathrm{T}}}$, and $\mathbf{N}_{\mathrm{R},n} \in \mathbb{C}^{N_{\mathrm{R}}\times 1}$ represent a channel matrix on the nth subcarrier between the relays and the terminal A, that between the relays and the terminal B, and the AWGN vector on the subcarrier, which are defined as $\mathbf{H}_{\mathrm{A},n} = \sum_{k=0}^{N_{\mathrm{F}}-1} \mathbf{H}_{\mathrm{A}}(k)\mathrm{e}^{-\mathrm{j}2\pi \frac{nk}{N_{\mathrm{F}}}}$, $\mathbf{H}_{\mathrm{B},n} = \sum_{k=0}^{N_{\mathrm{F}}-1} \mathbf{H}_{\mathrm{B}}(k)\mathrm{e}^{-\mathrm{j}2\pi \frac{nk}{N_{\mathrm{F}}}}$, and $\mathbf{N}_{\mathrm{R},n} = \frac{1}{\sqrt{N_{\mathrm{F}}}} \sum_{k=0}^{N_{\mathrm{F}}-1} \mathbf{N}_{\mathrm{R}}(k)\mathrm{e}^{-\mathrm{j}2\pi \frac{nk}{N_{\mathrm{F}}}}$. A rate one code is applied to the two modulation signal vectors, $\mathbf{S}_{\mathrm{A},n}$ and $\mathbf{S}_{\mathrm{B},n}$, at the relays. Let $\oplus$ denote encoding of the rate one code, an encoder output vector $\mathbf{S}_{\mathrm{R},n} \in \mathbb{C}^{N_{\mathrm{R}}\times 1}$ can be described as $\mathbf{S}_{\mathrm{R},n} = \mathbf{S}_{\mathrm{A},n} \oplus \mathbf{S}_{\mathrm{B},n}$. Because the modulation signal vectors are included in the received signal vector, the encoder output signal vector can be estimated from the received signal vector. Let $p(a|b)$ denote a conditional probability that an event a happens when an event b occurred, the encoder output signal vector can be estimated as,

$$\begin{aligned}\bar{\mathbf{S}}_{\mathrm{R},n} &= \arg\max_{\mathbf{S}_{\mathrm{R},n}} p\left(\mathbf{S}_{\mathrm{R},n}|\mathbf{Y}_{\mathrm{R},n}\right) \\ &= \arg\max_{\mathbf{S}_{\mathrm{R},n}=\mathbf{S}_{\mathrm{A},n}\oplus\mathbf{S}_{\mathrm{B},n}} p\left(\mathbf{S}_{\mathrm{A},n} \oplus \mathbf{S}_{\mathrm{B},n}|\mathbf{Y}_{\mathrm{R},n}\right). \end{aligned} \tag{5}$$

$\bar{\mathbf{S}}_{\mathrm{R},n} \in \mathbb{C}^{N_{\mathrm{R}}\times 1}$ in (5) represents an estimate of the encoder output vector $\mathbf{S}_{\mathrm{R},n}$. The estimated vector is defined as $\bar{\mathbf{S}}_{\mathrm{R},n} = (\bar{s}_{1,n} \cdots \bar{s}_{N_{\mathrm{R}},n})^{\mathrm{T}}$ where $\bar{s}_{i,n} \in \mathbb{C}$ denotes an estimated signal on the nth subcarrier at the ith relay. In every relay, the estimated encoder output signal is provided to the channel decoder via the deinterleaver, and the decoder output signal is modulated in the similar manner as that in the transmitters after the interleaving. All the relays convert the modulated signals in the frequency domain to the time domain signals as is usually done in systems with the OFDM.

In the next time slot, as is described above, all the relays simultaneously transmit the packets containing the time domain signals for the terminals. When a transmit time domain signal vector $\mathbf{X}_{\mathrm{R}}(k) \in \mathbb{C}^{N_{\mathrm{R}}\times 1}$ is defined as $\mathbf{X}_{\mathrm{R}}(k) = (x_1(k) \cdots x_{N_{\mathrm{R}}}(k))^{\mathrm{T}}$ where $x_i(k)$ represents a time domain signal transmitted from the ith relay, the packets are received at the terminal Ω, the kth signal of which is expressed as $\mathbf{Y}_{\Omega}(k) \in \mathbb{C}^{N_{\mathrm{T}}\times 1}$ in the following equation.

$$\mathbf{Y}_{\Omega}(k) = \mathbf{H}_{\Omega}^{\mathrm{H}}\mathbf{X}_{\mathrm{R}}(k) + \mathbf{N}_{\Omega}(k), \quad \Omega = \text{A or B} \tag{6}$$

$\mathbf{N}_{\Omega,n} \in \mathbb{C}^{N_{\mathrm{T}}\times 1}$ in (6) denotes the AWGN vector at the terminal Ω. As is indicated above, we assume the channel reciprocity between the link from the terminals to the relays, and that from the relays to the terminals in the relay

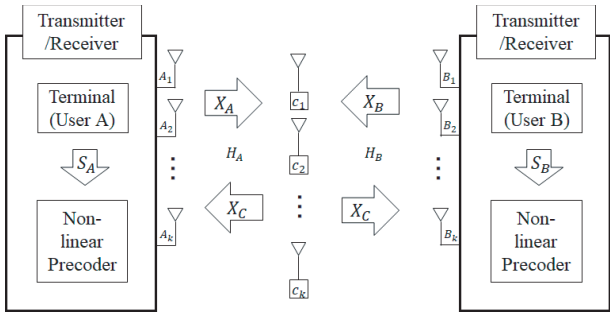

Fig. 1 Configuration of PLNC in 2-hop relay system.

system with TDD. The assumption is introduced for easy precoder implementation, while the assumption is not necessary for the signal detection at the terminals. As is seen in (6), since the system model is regarded as that in single user MIMO systems, conventional MIMO-OFDM detectors such as frequency domain minimum mean square error (MMSE) filters, can be applied to the receiver on the terminals for the signal detection. Let $\mathbf{X}_{\mathrm{R},n} \in \mathbb{C}^{N_\mathrm{R}\times 1}$ represent a modulation signal vector on the nth subcarrier that is defined as $\mathbf{X}_{\mathrm{R},n} = (x_{1,n}\cdots x_{N_\mathrm{R},n})^\mathrm{T}$, such a MIMO detector outputs an estimated modulation signal vector on the nth subcarrier, $\bar{\mathbf{X}}_{\mathrm{R},n} \in \mathbb{C}^{N_\mathrm{R}\times 1}$, where $\bar{\mathbf{X}}_{\mathrm{R},n}$ denotes an estimated vector of $\bar{\mathbf{X}}_{\mathrm{R},n}$. If $\tilde{\mathrm{A}}$ is defined as the other terminal for the terminal A, i.e., $\tilde{\mathrm{A}} = \mathrm{B}$, the modulation signal vector sent from the other terminal can be detected with the modulation signal vector sent from the own terminal in the first slot as,

$$\mathbf{S}_{\Omega,n} = \bar{\mathbf{X}}_{\mathrm{R},n} \ominus \mathbf{S}_{\tilde{\Omega},n}. \tag{7}$$

The system model is illustrated in Fig. 1. As is shown in the figure, we assume that the relays have no link to communicate each other, while communicating with the terminals.

Next section proposes coded modulation for the PLNC with the optimum precoder, which enables the relays to decode the received signal even when higher-order QAMs are applied.

3. Precoded PLNC With Coded Modulation

3.1 Coded Modulation for PLNC

We assume that 2^{2M}-QAM is applied to the system described in the previous section. Information bit stream is divided into two streams. When $N_\mathrm{P} \in \mathbb{N}$ represents the number of samples in a packet, i.e., packet length, the number of bits of the one stream is $N_\mathrm{R}N_\mathrm{F}N_\mathrm{P}M_\mathrm{H}$, and that of the other is $N_\mathrm{R}N_\mathrm{F}N_\mathrm{P}M_\mathrm{L}$ where $M_\mathrm{H} \in \mathbb{N}$ and $M_\mathrm{L} \in \mathbb{N}$ are defined as $M = M_\mathrm{L} + M_\mathrm{H}$. The latter bit stream is further divided into $N_\mathrm{R}N_\mathrm{F}$ streams. The $iN_\mathrm{F} + n$th stream is denoted as $B_{i,n}^{(\Omega_\mathrm{L})}$ where i and n represent a subcarrier number and an antenna number. Those $N_\mathrm{R}N_\mathrm{F}$ bit streams are fed to independent channel encoders with coding rate $R = \frac{1}{2}$, each of which is defined over the $\mathrm{GF}\left(2^{M_\mathrm{L}}\right)$ field where $\mathrm{GF}(q)$ denotes a Galois field with a modulus q. The same code is applied to those encoders in this paper. Let $G^{(\mathrm{L})}(D)$ represent a generator polynomial defined over the $\mathrm{GF}\left(2^{M_\mathrm{L}}\right)$ field where D denotes delay operator, the coded bit streams are obtained as follows.

$$\left(C_{\mathrm{I},i,n}^{(\Omega_\mathrm{L})}(D) \quad C_{\mathrm{Q},i,n}^{(\Omega_\mathrm{L})}(D)\right) = B_{i,n}^{(\Omega_\mathrm{L})}(D)\, G^{(\mathrm{L})}(D) \tag{8}$$

In (8), $C_{\mathrm{I},i,n}^{(\Omega_\mathrm{L})}(D)$ and $C_{\mathrm{Q},i,n}^{(\Omega_\mathrm{L})}(D)$ represent two symbol streams from the encoder. Every stream is provided to a symbol interleaver, and all the output streams from the interleavers $c_{\mathrm{I},i,n}^{(\Omega_\mathrm{L})} = \left(c_{\mathrm{I},i,n}^{(\Omega_\mathrm{L})}(0)\cdots c_{\mathrm{I},i,n}^{(\Omega_\mathrm{L})}(N_\mathrm{P}-1)\right) \in \mathbb{N}^{N_\mathrm{P}\times 1}$ and $c_{\mathrm{Q},i,n}^{(\Omega_\mathrm{L})} = \left(c_{\mathrm{Q},i,n}^{(\Omega_\mathrm{L})}(0)\cdots c_{\mathrm{Q},i,n}^{(\Omega_\mathrm{L})}(N_\mathrm{P}-1\right) \in \mathbb{N}^{N_\mathrm{P}\times 1}$ $i = 1\cdots N_\mathrm{R}$ $n = 1\cdots N_\mathrm{F}$ are fed to the QAM modulators.

On the other hand, the first bit stream is also encoded over the GF(2) filed with coding rate $R = \frac{1}{2}$, interleaved, and divided adequately into $2N_\mathrm{R}N_\mathrm{F}$ streams†. As a result, the $2N_\mathrm{R}N_\mathrm{F}$ streams are fed to the modulators. a pair of the first and the latter streams are denoted as $c_{\mathrm{I},i,n}^{(\Omega_\mathrm{H})} = \left(c_{\mathrm{I},i,n}^{(\Omega_\mathrm{H})}(0)\cdots c_{\mathrm{I},i,n}^{(\Omega_\mathrm{H})}(N_\mathrm{P}M_\mathrm{H}-1)\right) \in \mathbb{N}^{N_\mathrm{P}M_\mathrm{H}\times 1}$ and $c_{\mathrm{Q},i,n}^{(\Omega_\mathrm{H})} = \left(c_{\mathrm{Q},i,n}^{(\Omega_\mathrm{H})}(0)\cdots c_{\mathrm{Q},i,n}^{(\Omega_\mathrm{H})}(N_\mathrm{P}M_\mathrm{H}-1)\right) \in \mathbb{N}^{N_\mathrm{P}M_\mathrm{H}\times 1}$ $i = 1\cdots N_\mathrm{R}$ $n = 1\cdots N_\mathrm{F}$. With those bit streams, the QAM signals are defined as,

$$s_{\Omega_\mathrm{L},n,k}(i) = c_{\mathrm{I},i,n}^{(\Omega_\mathrm{L})}(k) + \mathrm{j}c_{\mathrm{Q},i,n}^{(\Omega_\mathrm{L})}(k), \tag{9}$$

$$s_{\Omega_\mathrm{H},n,k}(i) = \sum_{m=kM_\mathrm{H}}^{(k+1)M_\mathrm{H}-1}\left(c_{\mathrm{I},i,n}^{(\Omega_\mathrm{H})}(m) + \mathrm{j}c_{\mathrm{Q},i,n}^{(\Omega_\mathrm{H})}(m)\right)\, 2^{\mathrm{mod}[m,M_\mathrm{H}]+M_\mathrm{L}}, \tag{10}$$

$$s_{\Omega,n,k}(i) = \mathrm{BP}_M\left[s_{\Omega_\mathrm{L},n,k}(i) + s_{\Omega_\mathrm{H},n,k}(i)\right] \quad k = 0,\cdots,N_\mathrm{P}, \tag{11}$$

where $s_{\Omega,n,k}(i) \in \mathbb{C}$, $s_{\Omega_\mathrm{L},n,k}(i) \in \mathbb{C}$, and $s_{\Omega_\mathrm{H},n,k}(i) \in \mathbb{C}$ represent the kth modulation signal on the nth subcarrier sent for the ith relay, parts of the modulation signal $s_{\Omega,n,k}(i) \in \mathbb{C}$. In addition, $\mathrm{BP}_M[\alpha]$ represents a function that transfers a unipolar signal α to a bipolar signal, i.e., $\mathrm{BP}_M[\alpha] = 2\alpha - (1+\mathrm{j})\left(2^M - 1\right)$, and $\mathrm{mod}[a,b]$ denotes a function defined as $\mathrm{mod}[a,b] = a - \lfloor ab^{-1}\rfloor b$ with real numbers $a \in \mathbb{R}$ and $b \in \mathbb{R}$ where $\lfloor\bullet\rfloor$ denotes the floor function that outputs the nearest integer of the input. The proposed coded modulation is illustrated n Fig. 2. In the figure, the encoder defined over $\mathrm{GF}\left(2^{M_\mathrm{L}}\right)$ is employed at the ENC block in every MOD(i) block. The $iN_\mathrm{F} + n$th stream $B_{i,n}^{(\Omega_\mathrm{L})}$ containing $N_\mathrm{P}M_\mathrm{L}$ bits is fed to the encoder defined over the $\mathrm{GF}\left(2^{M_\mathrm{L}}\right)$ in $iN_\mathrm{F} + n$th modulator in the figure.

Because the same signal processing is applied to the signals in spite of the time index k in the proposed technique, the signals with the time index $k = 0$ are hereafter dealt as a representative in this paper. Because the attachment of 0 to the signals does not convey any information, the time index $k = 0$ is basically dropped from the signal notation, i.e.,

†Although any Galois field can be applied to the code, we use the $GF(2)$ filed to simplify the explanation and to show clearly the difference from the code over the $\mathrm{GF}\left(2^{M_\mathrm{L}}\right)$ field. The order of endowing, division, and interleaving can be changed. The optimum design of them is one of our future works.

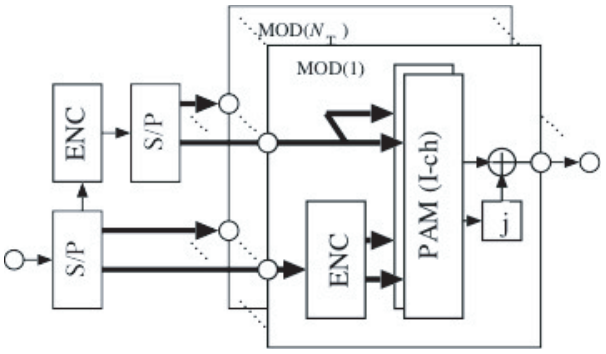

Fig. 2 Configuration of proposed coded modulation.

$s_{\Omega,n,k}(i) \Rightarrow s_{\Omega,n,0}(i) \Rightarrow s_{\Omega,n}(i)$. The modulation signal vector $\mathbf{S}_{\Omega,n} \in \mathbb{C}^{N_R \times 1}$ can be defined with the modulation signals as $\mathbf{S}_{\Omega,n} = (s_{\Omega,n}(1) \cdots s_{\Omega,n}(N_R))^T$.

3.2 Precoder Weight Optimization

We introduce a non-linear precoder with a feed forward filter and a feedback filter. Let $\mathbf{F}_{\Omega,n} \in \mathbb{C}^{N_R \times N_T}$ and $\mathbf{B}_{\Omega,n} \in \mathbb{C}^{N_R \times N_R}$ Ω =A or B denote weights for the feedforward filter and the feedback filter on the nth subcarrier, the precoder is defined as follows.

$$\mathbf{X}_{\Omega,n} = \mathbf{F}^H_{\Omega,n} \mathbf{V}_{\Omega,n} \tag{12}$$

$$\mathbf{S}_{\Omega,n} = \mathbf{B}^H_{\Omega,n} \mathbf{V}_{\Omega,n} - \mathbf{K}_{\Omega,n} L_d \tag{13}$$

In (13), $\mathbf{V}_{\Omega,n} \in \mathbb{C}^{N_R \times 1}$ represents an output from the feedback filter, where the elements of the Gaussian integer vector $\mathbf{K}_{\Omega,n}$ are determined through the feedback filtering. When the transmission signal vectors defined in (13) are simultaneously transmitted from the two terminals, the received signal vector on the nth subcarrier at all the relays can be rewritten as,

$$\mathbf{Y}_{R,n} = \mathbf{H}_{A,n} \mathbf{F}^H_{A,n} \mathbf{V}_{A,n} + \mathbf{H}_{B,n} \mathbf{F}^H_{B,n} \mathbf{V}_{B,n} + \mathbf{N}_{R,n}. \tag{14}$$

We define those weights that minimize the error between the received signals and the desired signals. As is proposed [22], it is the optimum to equalize the received signals from the two terminals on every subcarrier when QAMs are applied. The desired signal vector $\Xi_{R,n} \in \mathbb{C}^{N_R \times 1}$ on the nth subcarrier is defined as,

$$\Xi_{R,n} = \mathbf{S}_{A,n} + \mathbf{S}_{B,n} = \mathbf{B}^H_{A,n} \mathbf{V}_{A,n} + \mathbf{B}^H_{B,n} \mathbf{V}_{B,n}. \tag{15}$$

Even though the Gaussian integers are included as shown in (14), they are omitted because we assume that they can be removed with the modulo operation at the relays.

This paper proposes two precoding techniques to fulfill the above requirement, which are explained in the following.

3.2.1 Per Subcarrier Weight Optimization

When the desired signal vector is defined in (15), the error vector $\epsilon_n \in \mathbb{C}^{N_R \times 1}$ between the desired signal vector and the received signal vector on the nth subcarrier is defines as,

$$\epsilon_n = \Xi_{R,n} - g_n^{-1} \mathbf{Y}_{R,n}, \tag{16}$$

where $g_n \in \mathbb{R}$ denotes an equivalent gain of the nth subcarrier in the wireless channel. This means that the received signal power on one subcarrier is different from that on the other subcarriers. However, the sum transmission power of the two transmission signals on every subcarrier should be kept same whether or not precoding is applied, in order to maintain the power consumption of the terminals. The sum transmission power on the subcarrier is defined as,

$$\mathrm{E}\left[\left|\mathbf{X}_{A,n}\right|^2 + \left|\mathbf{X}_{B,n}\right|^2\right] = \mathrm{tr}\left[\mathbf{F}^H_{A,n} \mathbf{\Phi}_{A,n} \mathbf{F}_{A,n} + \mathbf{F}^H_{B,n} \mathbf{\Phi}_{B,n} \mathbf{F}_{B,n}\right] = P_S. \tag{17}$$

$P_S \in \mathbb{R}$, $\mathbf{\Phi}_{A,n} \in \mathbb{C}^{N_R \times N_R}$, and $\mathbf{\Phi}_{B,n} \in \mathbb{C}^{N_R \times N_R}$ in (17) denote transmission power, covariance matrices of the vector $\mathbf{V}_{\Omega,n}$ Ω = A and B, which are defined as $\mathbf{\Phi}_{\Omega,n} = \mathrm{E}\left[\mathbf{V}_{\Omega,n} \mathbf{V}^H_{\Omega,n}\right]$. The weight vector $\mathbf{W}_{\Omega,n}$ is optimized under constraint of the transmission power explained above. Hence, the optimum weight matrix is defined as a solution that minimizes the following cost function $J_n \in \mathbb{R}$ under constraint in (16). The closed form solution can be obtained with the method of Lagrange multiplier as,

$$J_n = \mathrm{tr}\left[\mathrm{E}\left[\epsilon_n \epsilon_n^H\right]\right] - \rho_n \Big(\mathrm{tr}\left[\mathbf{F}^H_{A,n} \mathbf{\Phi}_{A,n} \mathbf{F}_{A,n} + \mathbf{F}^H_{B,n} \mathbf{\Phi}_{B,n} \mathbf{F}_{B,n}\right] - P_S \Big). \tag{18}$$

In (18), ρ_n represents a Lagrange multiplier. After some manipulations, the optimum feedforward weight matrix can be derived as,

$$\mathbf{F}^H_{\Omega,n} = g_n \mathbf{H}^H_{\Omega,n} \left(\mathbf{H}_{\Omega,n} \mathbf{H}^H_{\Omega,n} - \rho_n g_n^2 \mathbf{I}_{N_R}\right)^{-1} \mathbf{B}^H_{\Omega,n}, \tag{19}$$

$$\rho_n g_n^2 = -\frac{\mathrm{tr}\left[\mathrm{E}\left[\mathbf{N}_{R,n} \mathbf{N}^H_{R,n}\right]\right]}{P_S} = -\frac{N_R \sigma^2}{P_S}, \tag{20}$$

where σ^2 indicates the variance of the AWGN. As is seen in (16), the power of the error vector ϵ_n is reduced as the gain g_n becomes large. Because the transmission power is restricted according to (17), if the condition number of the matrix in the parenthesis in the right hand of (19) is large, the gain g_n has to be set to a small value, which degrades the transmission performance. To reduce the condition number of the matrix, the lattice reduction is introduced. When the lattice reduction is applied, the channel matrix is transformed as,

$$\begin{pmatrix} \mathbf{H}^H_{\Omega,n} \\ \sqrt{-\rho_n g_n^2} \mathbf{I}_{N_R} \end{pmatrix} \mathbf{T}_{\Omega,n} = \mathbf{Q}_{\Omega,n} \mathbf{R}_{\Omega,n} = \mathbf{Q}_{\Omega,n} \mathbf{D}^{\frac{1}{2}}_{\Omega,n} \bar{\mathbf{R}}_{\Omega,n}. \tag{21}$$

$\mathbf{T}_{\Omega,n} \in \mathbb{C}^{N_R \times N_R}$, $\mathbf{Q}_{\Omega,n} \in \mathbb{C}^{(N_T+N_R) \times (N_T+N_R)}$, $\mathbf{R}_{\Omega,n} \in \mathbb{C}^{(N_T+N_R) \times N_R}$, $\mathbf{D}_{\Omega,n} \in \mathbb{C}^{N_R \times N_R}$, and $\bar{\mathbf{R}}_{\Omega,n} \in \mathbb{C}^{(N_T+N_R) \times N_R}$ denote a unimodular matrix, a unitary matrix, a right upper triangular matrix,

a diagonal matrix, and a right upper triangular matrix with the value of 1 in the diagonal positions. The two right upper triangular matrix $\mathbf{R}_{\Omega,n}$ and $\bar{\mathbf{R}}_{\Omega,n}$ are defined with the diagonal matrix $\mathbf{D}_{\Omega,n}$ as $\mathbf{R}_{\Omega,n} = \mathbf{D}_{\Omega,n}^{\frac{1}{2}}\bar{\mathbf{R}}_{\Omega,n}$. By substituting (21) for (19), and (12) and (13) for (2), the following can be derived as,

$$\mathbf{F}_{\Omega,n}^{\mathrm{H}} = g_n \mathbf{H}_{\Omega,n}^{\mathrm{H}} \mathbf{T}_{\Omega,n} \bar{\mathbf{R}}_{\Omega,n}^{-1} \mathbf{D}_{\Omega,n}^{-1}, \tag{22}$$

$$\mathbf{B}_{\Omega,n}^{\mathrm{H}} = \mathbf{T}_{\Omega,n}^{-\mathrm{H}} \bar{\mathbf{R}}_{\Omega,n}^{\mathrm{H}}, \tag{23}$$

When the feedback filter output vector $\mathbf{V}_{\Omega,n}$ is defined as $\mathbf{V}_{\Omega,n} = (v_{\Omega,n}(1) \cdots v_{\Omega,n}(N_{\mathrm{R}}))^{\mathrm{T}}$ where $v_{\Omega,n}(m) \in \mathbb{C}$ represents the mth entry, the feedback filter output vector can be obtained serially as is done in THPs, by taking account of (13) and (23).

$$v_{\Omega,n}(m) = \left\lfloor \frac{\mathrm{cmod}\left[\mathbf{T}_{\Omega,n}^{(m)\,\mathrm{H}} \mathbf{S}_{\Omega,n} - \sum_{k=m+1}^{N_{\mathrm{R}}} \bar{r}_{\Omega,n}(k,m)^{*}\, v_{\Omega,n}(k), L_{\mathrm{d}}\right]}{\bar{r}_{\Omega,n}(m,m)} \right\rfloor$$
$$m = 1, \cdots, N_{\mathrm{R}} \tag{24}$$

In (24), $\mathbf{T}_{\Omega,n}^{(m)} \in \mathbb{C}^{N_{\mathrm{R}}\times 1}$, and $\bar{r}_{\Omega,n}(k,m) \in \mathbb{R}$ denote the mth column vector of the unimodular matrix defined as $\mathbf{T}_{\Omega,n} = \left(\mathbf{T}_{\Omega,n}^{(1)} \cdots \mathbf{T}_{\Omega,n}^{(N_{\mathrm{R}})}\right)$, and the (k,m) entry of the matrix $\bar{\mathbf{R}}_{\Omega,n}$. In addition, let $\alpha \in \mathbb{C}$ denote a complex number defined with real numbers $\alpha_{\mathrm{R}} \in \mathbb{R}$ and $\alpha_{\mathrm{I}} \in \mathbb{R}$ as $\alpha = \alpha_{\mathrm{R}} + \mathrm{j}\alpha_{\mathrm{I}}$, $\mathrm{cmod}[\alpha, L_{\mathrm{d}}]$ indicates a function defined as $\mathrm{cmod}[\alpha, L_{\mathrm{d}}] = \mathrm{rmod}[\alpha_{\mathrm{R}}, L_{\mathrm{d}}] + \mathrm{j}\ \mathrm{rmod}[\alpha_{\mathrm{I}}, L_{\mathrm{d}}]$ where $\mathrm{rmod}[\alpha_{\mathrm{I}}, L_{\mathrm{d}}]$ represents a function defined as $\mathrm{rmod}[\alpha_{\mathrm{I}}, L_{\mathrm{d}}] = \alpha_{\mathrm{I}} - \lfloor \frac{\alpha_{\mathrm{I}}}{L_{\mathrm{d}}} + \frac{1}{2} \rfloor L_{\mathrm{d}}$. On the other hand, the gain g_n fulfilling the requirement (17) can be obtained as,

$$g_n = \sqrt{\frac{6P_{\mathrm{S}}}{L_{\mathrm{d}}^2 \left(\mathrm{tr}\left[\sum_{\Omega=\mathrm{A}}^{\mathrm{B}} \mathbf{H}_{\Omega,n}^{\mathrm{H}} \mathbf{T}_{\Omega,n} \bar{\mathbf{R}}_{\Omega,n}^{-1} \mathbf{D}_{\Omega,n}^{-1} \bar{\mathbf{R}}_{\Omega,n}^{-\mathrm{H}} \mathbf{T}_{\Omega,n}^{\mathrm{H}} \mathbf{H}_{\Omega,n} \right] \right)}}. \tag{25}$$

In the above derivation, we apply an approximation that $\mathbf{\Phi}_{\mathrm{A},n} = \mathbf{\Phi}_{\mathrm{B},n} = \sigma_v^2 \mathbf{I}_{N_{\mathrm{T}}}$ where $\sigma_v^2 = \frac{1}{6} L_{\mathrm{d}}^2$.

3.2.2 Total Weight Optimization

While the sum transmission power on every subcarrier is restricted in the technique proposed above, it is enough to keep the sum transmission power of all the subcarriers from the view point of power consumption of terminals. In a word, the transmission power constraint can be described as,

$$\mathrm{E}\left[|\mathbf{X}_{\mathrm{A}}(k)|^2 + |\mathbf{X}_{\mathrm{B}}(k)|^2\right] = \sum_{n=0}^{N_{\mathrm{F}}-1} \mathrm{tr}\left[\mathbf{F}_{\mathrm{A},n}^{\mathrm{H}} \mathbf{\Phi}_{\mathrm{A},n} \mathbf{F}_{\mathrm{A},n} + \mathbf{F}_{\mathrm{B},n}^{\mathrm{H}} \mathbf{\Phi}_{\mathrm{B},n} \mathbf{F}_{\mathrm{B},n}\right] = P_{\mathrm{T}}, \tag{26}$$

where $P_{\mathrm{T}} \in \mathbb{R}$ indicates transmission power defined as $P_{\mathrm{T}} = P_{\mathrm{S}} N_{\mathrm{F}}$. Because the transmission power constraint is defined in the time domain as shown in (26), an error vector between the desired signal vector and the received signal vector can be also defined in the time domain as,

$$\epsilon(k) = \sum_{n=0}^{N_{\mathrm{F}}-1} \Xi_{\mathrm{R},n} \mathrm{e}^{-\mathrm{j}2\pi \frac{kn}{N_{\mathrm{F}}}} - g^{-1} \mathbf{Y}_{\mathrm{R}}(k). \tag{27}$$

In (27), $\epsilon(k) \in \mathbb{C}^{N_{\mathrm{R}}\times 1}$ and $g \in \mathbb{R}$ denote the error vector and an equivalent gain of the transmission signals in the wireless channel. With the error vector and the power constraint, the optimum weight vectors can be defined as a solution to minimize the following cost function $J \in \mathbb{R}$ under constraint in (26). The optimum weight can be obtained with the method of Lagrange multiplier.

$$J = \mathrm{tr}\left[\mathrm{E}\left[\boldsymbol{\varepsilon}(k)\,\boldsymbol{\varepsilon}(k)^{\mathrm{H}}\right]\right] - \rho\left(\sum_{n=0}^{N_{\mathrm{F}}-1} \mathrm{tr}\left[\mathbf{F}_{\mathrm{A},n}^{\mathrm{H}} \mathbf{\Phi}_{\mathrm{A},n} \mathbf{F}_{\mathrm{A},n} + \mathbf{F}_{\mathrm{B},n}^{\mathrm{H}} \mathbf{\Phi}_{\mathrm{B},n} \mathbf{F}_{\mathrm{B},n}\right] - P_{\mathrm{T}}\right) \tag{28}$$

In (28), $\rho \in \mathbb{C}$ represents a Lagrange multiplier. By similar mathematical manipulation as that in the previous section, the feedforward filter and the gain are also obtained as,

$$\mathbf{F}_{\Omega,n}^{\mathrm{H}} = g \mathbf{H}_{\Omega,n}^{\mathrm{H}} \left(\mathbf{H}_{\Omega,n} \mathbf{H}_{\Omega,n}^{\mathrm{H}} - \rho g^2 \mathbf{I}_{N_{\mathrm{R}}}\right)^{-1} \mathbf{B}_{\Omega,n}^{\mathrm{H}}, \tag{29}$$

$$\rho g^2 = -\frac{\mathrm{tr}\left[\mathrm{E}\left[\mathbf{N}_{\mathrm{R}}(k) \mathbf{N}(k)^{\mathrm{H}}\right]\right]}{P_{\mathrm{x}}} = -\frac{2N_{\mathrm{R}}\sigma^2}{P_{\mathrm{T}}}. \tag{30}$$

While the weight matrix in (29) and ρg^2 in (30) are reduced to the similar ones in (19) and (20) respectively, the gain g fulfilling the requirement (26) can be derived as,

$$g = \sqrt{\frac{6P_{\mathrm{T}}}{L_{\mathrm{d}}^2 \left(\mathrm{tr}\left[\sum_{\Omega=\mathrm{A}}^{\mathrm{B}} \sum_{n=0}^{N_{\mathrm{F}}-1} \mathbf{H}_{\Omega,n}^{\mathrm{H}} \mathbf{T}_{\Omega,n} \bar{\mathbf{R}}_{\Omega,n}^{-1} \mathbf{D}_{\Omega,n}^{-1} \bar{\mathbf{R}}_{\Omega,n}^{-\mathrm{H}} \mathbf{T}_{\Omega,n}^{\mathrm{H}} \mathbf{H}_{\Omega,n} \right] \right)}}. \tag{31}$$

The denominator in the parenthesis in (31) contains the channel matrices on all the subcarriers, while that in (25) consists of only the channel matrices on the nth subcarrier. If the denominator in (25) gets small, the gain g_n will become small, which degrades the transmission performance. On the other hand, because the denominator in (31) has more terms than that in (25), the gain g gets faded with smaller probability than g_n.

3.3 Soft Decoding at Relay

As is inferred by (15) and (16), the received signal vector at the relays is expected to be a weight sum of the two transmit signals with the common weight of the gain g_n[†]. Although the Gaussian integer multiples added by the modulo function by the precoder and the bias constant used to transfer

[†]Even though The same explanation is also valid for the proposed PLNC with the total weight optimization, we explain decoding in the proposed PLNC with the per subcarrier weight optimization as an example.

unipolar signals to bipolar signals are included in the received subcarrier signals, they can be easily removed with modulo functions and bias adjustment from the received signals at the relays. If they are removed, the received signal vector on the nth subcarrier $\tilde{\mathbf{Y}}_{\mathrm{R},n} \in \mathbb{C}^{N_\mathrm{R}\times 1}$ will be generated, which can be expressed as,

$$\tilde{\mathbf{Y}}_{\mathrm{R},n} \simeq g_n \left(\mathbf{S}_{\mathrm{A},n} + \mathbf{S}_{\mathrm{B},n}\right) + \mathbf{N}_{\mathrm{R},n}. \tag{32}$$

Let $\tilde{y}_{\mathrm{R},n}(m) \in \mathbb{C}$ represent the mth entry of the vector $\tilde{\mathbf{Y}}_{\mathrm{R},n}$, i.e., $\tilde{\mathbf{Y}}_{\mathrm{R},n} = (\tilde{y}_{\mathrm{R},n}(1) \cdots \tilde{y}_{\mathrm{R},n}(N_\mathrm{R}))^\mathrm{T}$, the entry $\tilde{y}_{\mathrm{R},n}(m)$ can be written as,

$$\begin{aligned}\tilde{y}_{\mathrm{R},n}(i) = g_n \sum_{\Omega=\mathrm{A}}^{\mathrm{B}} \left(c_{\mathrm{I},i,n}^{(\Omega_\mathrm{L})} + \mathrm{j}c_{\mathrm{Q},i,n}^{(\Omega_\mathrm{L})}\right) \\ + g_n \sum_{\Omega=\mathrm{A}}^{\mathrm{B}} \sum_{m=0}^{M_\mathrm{H}-1} \left(c_{\mathrm{I},i,n}^{(\Omega_\mathrm{H})}(m) + \mathrm{j}c_{\mathrm{Q},i,n}^{(\Omega_\mathrm{H})}(m)\right) 2^{m+M_\mathrm{L}} \\ + \mathbf{N}_{\mathrm{R},n}.\end{aligned} \tag{33}$$

Because the sum of the two code words is one of the code words over GF(2^{M_L}), the sum can be decoded at the relays. When convolutional codes over GF(2^{M_L}) is applied, for example, the state transition $B_{t_1} \rightarrow B_{t_2}$ is assumed to generate a code word $(c_{\mathrm{I},(t_{1\to 2})} \quad c_{\mathrm{Q},(t_{1\to 2})})$. The code words that satisfy the following equation are defined as $c_{\Upsilon,i,n,(t_{1\to 2})}^{(\Omega_\mathrm{L})}$ Υ = I, Q, Ω = A, B as,

$$\begin{pmatrix} \mathrm{mod}\left[c_{\mathrm{I},i,n,(t_{1\to 2})}^{(\mathrm{A_L})} + c_{\mathrm{I},i,n,(t_{1\to 2})}^{(\mathrm{B_L})}, 2^{M_\mathrm{L}}\right] \\ \mathrm{mod}\left[c_{\mathrm{Q},i,n,(t_{1\to 2})}^{(\mathrm{A_L})} + c_{\mathrm{Q},i,n,(t_{1\to 2})}^{(\mathrm{B_L})}, 2^{M_\mathrm{L}}\right] \end{pmatrix}^\mathrm{T} = \begin{pmatrix} c_{\mathrm{I},(t_{1\to 2})} \\ c_{\mathrm{Q},(t_{1\to 2})} \end{pmatrix}^\mathrm{T}. \tag{34}$$

Because mod [•] is included in (34), multiple code words $c_{\Upsilon,i,n,(t_{1\to 2})}^{(\Omega_\mathrm{L})}$ Υ = I, Q, Ω = A, B may satisfy the above equation, even if the terms in the left hand side are fixed. This means that a part of the received signal is a code word of the code over GF(2^{M_L}), which is decoded by the proposed soft decoding.

On the other hand, if two QAM signals are added, the added signal is on the grid. Therefore, a part of the second term in the right hand side of (33) can be expressed as $\sum_{\Omega=\mathrm{A}}^{\mathrm{B}} \sum_{m=0}^{M_\mathrm{H}-1} \left(c_{\mathrm{I},i,n,(\mathrm{t}_{1\to 2})}^{(\Omega_\mathrm{H})}(m) + \mathrm{j}c_{\mathrm{Q},i,n,(\mathrm{t}_{1\to 2})}^{(\Omega_\mathrm{H})}(m)\right) 2^m = \sum_{m=0}^{M_\mathrm{H}} (a_{\mathrm{I},i,n}(m) + \mathrm{j}a_{\mathrm{Q},i,n}(m)) \ 2^m$ where $a_{\Upsilon,i,n}(m)$ takes 1 or 0. In the proposed soft decoding, the second term in the right hand side of (33) is firstly estimated.

$$\begin{aligned}\left\{a_{\Upsilon,i,n,(t_{1\to 2})}(m) \mid m = 0, \cdots, M_\mathrm{H}, \Upsilon = \mathrm{I},\ \mathrm{Q}\right\} \\ = \arg\min_{a_{\Upsilon,i,n}(m)} \left\| g_n^{-1}\tilde{y}_{\mathrm{R},n}(i) - \sum_{\Omega=\mathrm{A}}^{\mathrm{B}} \left(c_{\mathrm{I},i,n,(t_{1\to 2})}^{(\Omega_\mathrm{L})} + \mathrm{j}c_{\mathrm{Q},i,n,(t_{1\to 2})}^{(\Omega_\mathrm{L})}\right) \right. \\ \left. + \sum_{m=0}^{M_\mathrm{H}} (a_{\mathrm{I},i,n}(m) + \mathrm{j}a_{\mathrm{Q},i,n}(m)) \ 2^{m+M_\mathrm{L}} \right\|^2\end{aligned} \tag{35}$$

As is shown in (35), the two QAM signals are not estimated but the added signal on the grid point is estimated. In a word, it is not minded how $a_{\Upsilon,i,n,(t_{1\to 2})}(m)$ is made from $c_{\mathrm{I},i,n,(t_{1\to 2})}^{(\mathrm{A_L})}$ and $c_{\mathrm{Q},i,n,(t_{1\to 2})}^{(\mathrm{A_L})}$. Although the maximum likelihood estimation is performed, the estimation is easily carried out with the region detection, because the signal is located on the grid. Because there are multiple code words satisfying (34) as described above, the metric $\beta_{\mathrm{R},i,n,(t_{1\to 2})}$ corresponding to the state transmission $B_{t_1} \rightarrow B_{t_2}$ can be estimated as follows.

$$\begin{aligned}\beta_{\mathrm{R},i,n,(t_{1\to 2})} = \min_{c_{\Upsilon,i,n,(t_{1\to 2})}^{(\Omega_\mathrm{L})}} \left| \tilde{y}_{\mathrm{R},n}(i) - g_n \sum_{\Omega=\mathrm{A}}^{\mathrm{B}} \left(c_{\mathrm{I},i,n,(t_{l\to 2})}^{(\Omega_\mathrm{L})} + \mathrm{j}c_{\mathrm{Q},i,n,(t_{l\to 2})}^{(\Omega_\mathrm{L})}\right) \right. \\ \left. + g_n \sum_{m=0}^{M_\mathrm{H}} (a_{\mathrm{I},i,n,(\mathrm{t}_{1\to 2})}(m) + \mathrm{j}a_{\mathrm{Q},i,n,(t_{l\to 2})}(m)) \ 2^{\mathrm{mod}[m,M_\mathrm{H}]+M_\mathrm{L}} \right|^2\end{aligned} \tag{36}$$

The proposed soft decoding is carried out with the branch metric defined in (36).

4. Computer Simulation

The performance of the proposed PLNC is evaluated in a MIMO-OFDM two-hop bi-directional relay system where 4 relays with one antenna is placed between two terminals with 4 antennas, i.e, $(N_\mathrm{T}, N_\mathrm{R}) = (4, 4)$. 3-path Rayleigh fading based on the Jakes' model [25] is applied as a channel model between every pair of the transmit antenna and the receive antenna. Although any QAM can be applied, the 16QAM and the 256QAM are utilized for the performance evaluation. The LLL algorithm is used for the lattice reduction [26], [27]. When the 256QAM is applied, $M = 4$ is divided into $M_\mathrm{H} = 3$ and $M_\mathrm{L} = 1$, while the setting of $M_\mathrm{H} = 1$ and $M_\mathrm{L} = 1$ is used in the proposed system with the 16QAM. GF (2) convolutional code [28] is used in the performance evaluation. In a word, the convolutional code over the GF(2^L) is reduced to that over the binary field. In general, the decoding complexity increases exponentially as the M_L of the GF$\left(2^{M_\mathrm{L}}\right)$ becomes long when convolutional codes defined over the GF$\left(2^{M_\mathrm{L}}\right)$ are applied. Because this is a first step of the research, we stated the research with simple configuration for confirming the basic performance of the proposed technique. Main parameters are summarized in Table 1. While the precoder with the lattice reduction is explained above, the lattice reduction can be replaced with the sorted QR decomposition (SQRD). If the unimodular matrix $\mathbf{T}_{\Omega,n}$ is replaced with the permutation matrix generated in the SQRD, the SQRD based precoder is obtained [24]. Since that configuration is also regarded as one realization of the proposed precoder, the performance of them is compared in the following.

4.1 Coding Gain

The performance of the proposed PLNC is shown in Fig. 3. The BER performance at the relays is evaluated when the 16QAM and the total weight optimization are applied to

Table 1 Parameter in computer simulation.

No. of antennas on a terminal N_T	4
No. of antennas on a relay	1
No. of relays N_R	4
Modulation	16QAM, 256QAM/OFDM
No. of subcarriers	64
Channel model	3-path Rayleigh fading
Lattice reduction	LLL algorithm with $\delta = 0.75$
(M_H, M_L)	(1, 1) in 16QAM, (3, 1) in 256QAM
Channel coding	Convolutional code $(K = 3, R = \frac{1}{2})$

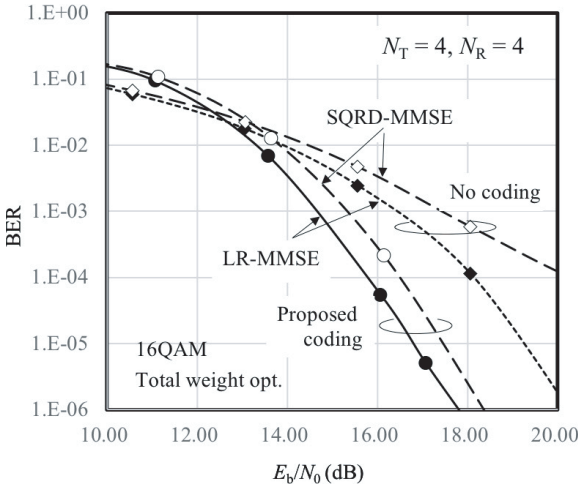

Fig. 3 BER comparison (16QAM).

the proposed precoding. In the figure, "LR-MMSE" and "SQRD-MMSE" denote the proposed precoding with the lattice reduction and the SQRD, respectively. The performance without decoding at the relays is added in the figure as a reference. The proposed PLNC achieves a coding gain of about 2 dB at the BER of 10^{-4} when the lattice reduction is used, while a coding gain of about 4 dB is attained at the same BER when the SQRD is used[†].

Figure 4 shows the performance of the proposed PLNC when the 256QAM is used. The total weight optimization is also applied in the figure. The proposed PLNC achieves a coding gain of about 2 dB at the BER of 10^{-4} when the lattice reduction is used. When the SQRD is applied, the performance is greatly degraded from that of the PLNC with the lattice reduction. In contrast, the PLNC with the lattice reduction achieves a more than 4-branch diversity gain despite of modulation schemes.

[†]As is described in Table 1, the LLL algorithm is applied for the lattice reduction. Both the LLL algorithm and the SQRD decompose the input matrix into an upper triangular matrix and unitary matrix. Although the SQRD only tries to arrange the diagonal elements in ascending order, the SQRD can't guarantee the perfect arrangement. On the other hand, the LLL algorithm achieves the semi orthogonal condition by iterative signal processing [26]. We understand that the LLL algorithm is better because the LLL achieves the condition while the SQRD can' guarantee the rearrangement. We understand that this is the reason why the LLL outperforms the SQRD.

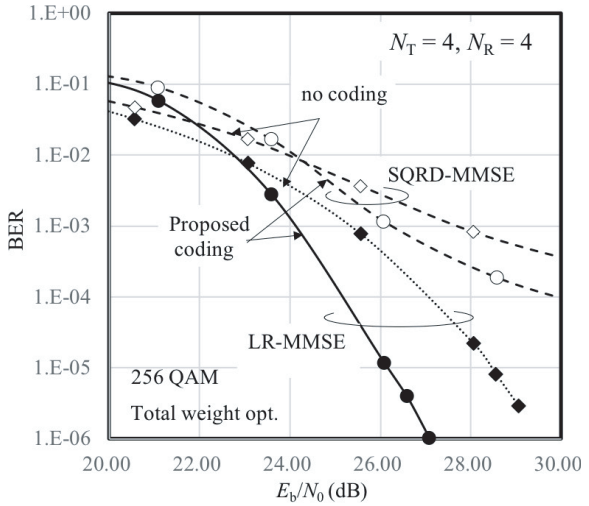

Fig. 4 BER comparison (256QAM).

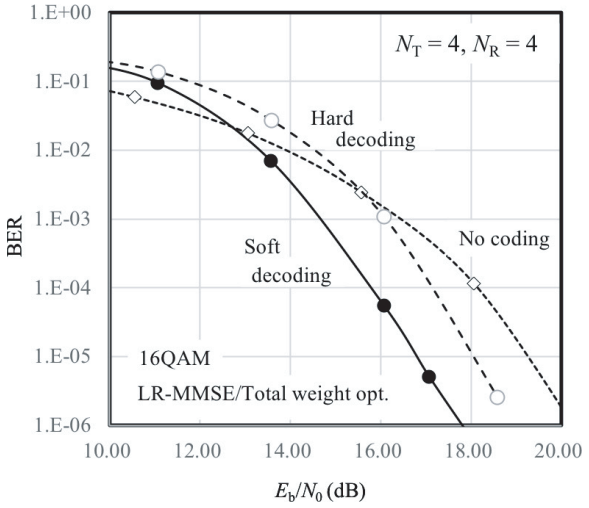

Fig. 5 Soft vs. hard decoding (16QAM).

4.2 Soft Decoding Gain

Figure 5 compares the coding gain of the proposed soft decoding and that of the hard decoding, when the 16QAM is applied. The same performance comparison is made in Fig. 6 where the 256QAM is used. The total weight optimization and the lattice reduction are applied to the proposed precoding in the both figures. The soft decoding attains a gain of about 1.5 dB at the BER of 10^{-4} in the both figures.

4.3 SNR Performance of Proposed PLNC

As is shown in Fig. 3 and Fig. 4, the proposed precoding with the lattice reduction achieves the better performance than that with the SQRD. The performance is confirmed in term of the signal to noise power ratio (SNR) in Fig. 7. The cumulative distribution function with respect to the

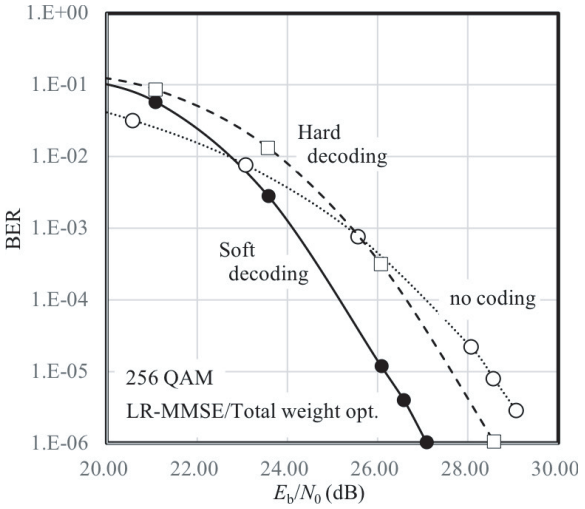

Fig. 6 Soft vs. hard decoding (256QAM).

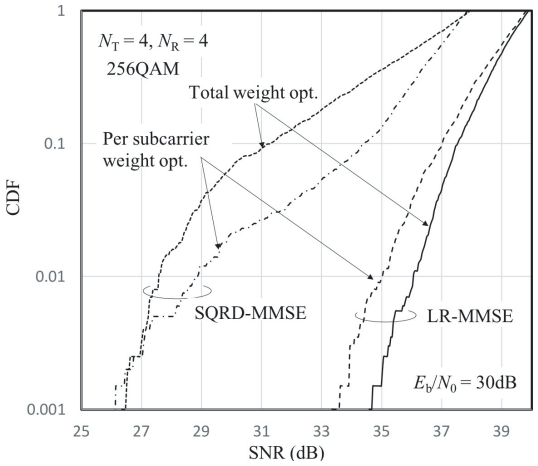

Fig. 7 CDF of signals received at relays.

SNR of the decoder input signals is shown in the figure. The 256QAM is applied and the average E_b/N_0 is set as $E_b/N_0 = 30$ dB. The precoding with the lattice reduction achieves much better performance than that with the SQRD, which agrees with the performances shown in Fig. 4. Especially, the probability that the SNR is less than 30 dB is more than 1% when the SQRD is used, while the probability that the SNR gets smaller than 33 dB is less than 0.1% when the lattice reduction is employed. Because the proposed precoding is based on the MMSE criterion, the performance depends on the distribution of the equivalent gain g_n. In general, the BER is more improved as the distribution becomes concentrated at a higher value. Because the LLL algorithm is better than the SQRD, hence, the LLL algorithm makes the distribution of the equivalent gain g_n more concentrated than the SQRD. As is defined in (25) and (31), on the other hand, the total weight optimization equalizes the SNR performances of all the streams, while the per subcarrier weight optimization does not. Therefore, even if the LLL algorithm concentrates the distribution of the equivalent gain g_n as much as possible, the per subcarrier weight optimization let let the small equivalent gain g_n. The SNR distribution of the per subcarrier weight optimization is a little bit inferior to that of the other when the LLL algorithm is applied [†]. This is the reason why the LLL with the total weight optimization algorithm achieves the best performance among the other combination. Because the BER performance is more degraded with small SNR as higher-order modulations are used. Therefore, the SQRD degrades the BER performance more seriously in the system with the 256QAM than in that with the 16QAM, compared with the lattice reduction. This analysis agrees with the large performance gap between the system with SQRD and that with the lattice reduction shown in Fig. 4.

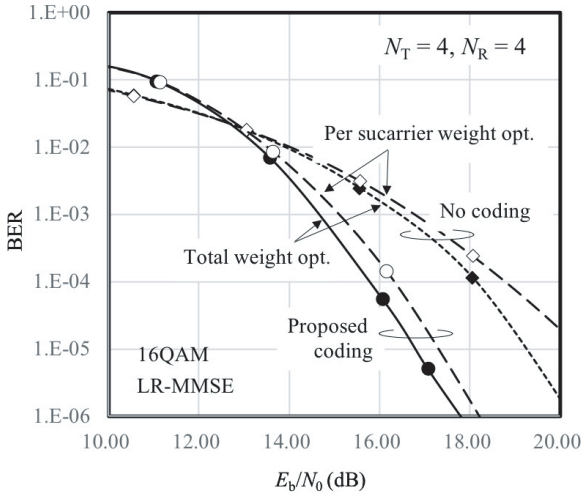

Fig. 8 Total vs. subcarrier weight optimization (16QAM).

In addition, Fig. 7 infers that the total power optimization achieves better BER performance than the per subcarrier weight optimization, when the LLL algorithm is applied.

4.4 Performance Comparison of Proposed Weight Optimization Techniques

Figure 8 compares the per subcarrier weight optimization and the total power optimization in terms of the BER when the 16QAM and the lattice reduction are used. They are also compared in Fig. 9 where the 256QAM is used. As is suggested in Fig. 7, the total weight optimization achieves about 0.5 dB better BER performance than the per subcarrier weight optimization when the 16QAM is used. The performance gap between the total weight optimization the per subcarrier weight optimization is increased to about 1.0 dB when the 256QAM is used. The performance gain gets higher as higher-order modulation schemes are applied due to the same reason why the SQRD degrades the performance more seriously in the system with higher-order modulation

[†]It is one of our future tasks to analyze the reason why the per subcarrier weight control to outperform the total weight control in terms of the SNR when the SQRD is applied.

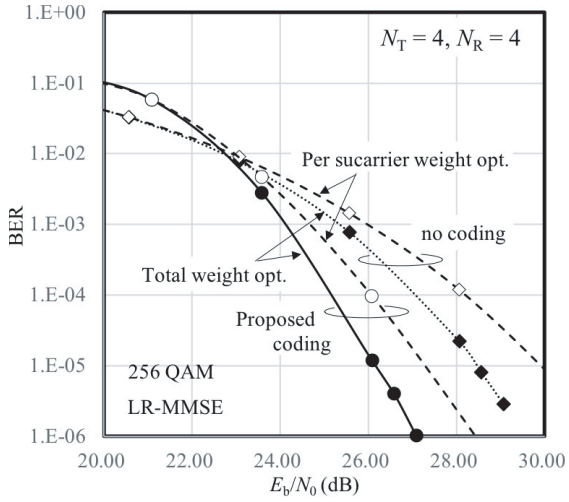

Fig. 9 Total vs. subcarrier weight optimization (256QAM).

schemes.

5. Conclusion

This paper proposes precoded PLNC with coded modulation for MIMO-OFDM bi-directional wireless relay systems. The proposed coded modulation enables the relays to decode the signals even in the system where higher-order QAMs are employed. Furthermore, we have proposed a technique to implement soft decoding in the PLNC. We have proposed two weight optimization techniques for the precoding for the system. The one is named as per subcarrier weight optimization where the weight is defined in every subcarrier. The other is called as total power optimization where the weight is optimized in the time domain. The configuration of the precoding with the lattice reduction is shown as one realization of the proposed precoder.

The performance of the proposed PLNC is evaluated by computer simulation in a MIMO-OFDM two-hop bi-directional wireless relay system where 4 relays with one antenna are surrounded by the two terminals with 4 antennas. The soft input decoding attains a coding gain of about 2 dB at the BER of 10^{-4} in the system not only with the 16QAM but also with the 256QAM. On the other hand, the total weight optimization achieves about 1.0 dB better BER performance than the other when the 256QAM is employed.

Acknowledgments

This work has been supported by JSPS KAKENHI Grant Number JP18K04142 and NTT DoCoMo, Co. Ltd.

References

[1] P. Popovski and H. Yomo, "Physical network coding in two way wireless relay channels," IEEE ICC, 2007.
[2] R.H.Y. Louie, Y. Li, and B. Vucetic, "Practical physical layer network coding for two-way relay channels: Performance analysis and comparison," IEEE Trans. Wireless Commun., vol.9, no.2, pp.764–777, 2010.
[3] R.H.Y. Louie, Y. Li, and B. Vucetic, "Performance analysis of physical layer network coding in two-way relay channels," IEEE GLOBECOM, 2009.
[4] M. Ju and I.-M. Kim, "Error performance analysis of BPSK modulation in physical-Layer network-coded bidirectional relay networks," IEEE Trans. Commun., vol.58, no.10, pp.2770–2775, 2010.
[5] V.T. Muralidharan and B.S. Rajan, "Performance analysis of adaptive physical layer network coding for wireless tow-way relaying," IEEE PIMRC, 2012.
[6] H. Gao, T. Lv, S. Zhang, C. Yuen, and S. Yang, "Zero-forcing based MIMO two-way relay with relay antenna selection: Transmission scheme and diversity analysis," IEEE Trans. Wireless Commun., vol.11, no.12, pp.4426–4437, 2012.
[7] M. Eslamifar, W.H. Chin, C. Yuen, and Y.L. Guan, "Performance analysis of two-step bi-directional relaying with multiple antennas," IEEE Trans. Wireless Commun., vol.11, no.12, pp.4237–4242, 2012.
[8] L. Shi, T. Yang, K. Cai, P. Chen, and T. Guo, "On MIMO linear physical layer network coding: Full-rate full-diversity design and optimization," IEEE Trans. Wireless Commun., vol.17, no.5, pp.3498–3511, 2018.
[9] C. Hausl and J. Hagenauer, "Iterative network and channel decoding for the two-way relay channel," IEEE ICC, pp.1568–1573, 2006.
[10] S. Zhang and S.-C. Liew, "Channel coding and decoding in a relay system operated with physical-layer network coding," IEEE J. Sel. Areas Commun., vol.27, no.5, pp.788–796, 2009.
[11] U. Bhat and T.M. Duman, "Decoding strategies at the relay with physical-layer network coding," IEEE Trans. Wireless Commun., vol.11, no.12, pp.4503–4513, 2012.
[12] P. Chen, S.C. Liew, and L. Shi, "Bandwidth-efficient coded modulation schemes for physical-layer network coding with high-order modulations," IEEE Trans. Commun., vol.65, no.1, pp.147–160, Jan. 2017.
[13] L. Yang, T. Yang, Y. Xie, J. Yuan, and J. An, "Linear physical-layer network coding and information combining for the K-user fading multiple-access relay network," IEEE Trans. Wireless Commun., vol.15, no.8, pp.5637–5650, 2016.
[14] D. Fang, A. Burr, and J. Yuan, "Linear physical-layer network coding over hybrid finite ring for Rayleigh fading two-way relay channels," IEEE Trans. Commun., vol.62, no.9, pp.3249–3261, Jan. 2014.
[15] R.F. H. Fischer, Precoding and Signal Processing for Digital Transmission, Willey-IEEE Press, 2002.
[16] Y.-T. Kim, K. Lee, M. Park, K.-J. Lee, and I. Lee "Precoding designs based on minimum distance for two-way relaying MIMO systems with physical network coding," IEEE Trans. Commun., vol.6, no.10, pp.4151–4160, Oct. 2013.
[17] S. Denno and D. Umehara, "Simplified maximum likelihood detection with unitary precoding for XOR physical layer network coding," IEICE Trans. Commun., vol.E100-B, no.1, pp.167–176, Jan. 2017.
[18] H. Harashima and H. Miyakawa, "Matched-transmission technique for channels with intersymbol interference," IEEE Trans. Commun., vol.20, no.4, pp.774–780, 1972.
[19] M. Tomlinson, "New automatic equaliser employing modulo arithmetic," Electron. Lett., vol.7, no.5/6, pp.138–139, March 1971.
[20] E.C.Y. Peh and Y.-C. Liang, "Power and modulo loss tradeoff with expanded soft demapper for LDPC coded GMD-THP MIMO systems," IEEE Trans. Wireless Commun., vol.8, no.2, pp.714–724, 2009.
[21] A.G.-Rodriguez and C. Masouros, "Power-efficient Tomlinson-Harashima precoding for the downlink of multi-user MISO systems," IEEE Trans. Commun., vol.62, no.6, pp.1884–1896, 2014.
[22] S. Denno, Y. Nagai, and Y. Hou, "XOR physical kayer network coding with non-linear precoding for quadrature amplitude modulations in bi-directional MIMO relay systems," IEICE Trans. Com-

mun., vol.E102-B, no.10, pp.2073–2081, Oct. 2019.
[23] B.M. Hochwald, C.B. Peel and A.L. Swindlehurst, "A vector-perturbation technique for near-capacity multiantenna multiuser communication — Part II: Perturbation," IEEE Trans. Commun., no.53, vol.3, pp.537–544, 2005.
[24] K. Kusume, M. Joham, W. Utschick, and G. Bauch, "Cholesky factorization with symmetric permutation applied to detecting and precoding spatially multiplexed data streams," IEEE Trans. Signal. Process., vol.55, no.6, pp.3089–3103, 2007.
[25] W.C. Jakes, Microwave Mobile Communications, IEEE Press, 1994.
[26] A.K. Lenstra, H.W. Lenstra, Jr., and L. Lovasz, "Factoring polynomials with rational coefficients," Math. Ann., vol.261, pp.515–534, 1982.
[27] D. Wübben, R. Böhnke, V. Kühn, and K. Kammeyer, "Near-maximum-likelihood detection of MIMO systems using MMSE-based lattice-reduction," Proc. IEEE ICC 2004, vol.2, pp.798–802. Paris, France, 2004.
[28] J.G. Proakis, Digital Communications, 5th ed., McGraw-Hill, 2008.

Satoshi Denno received the M.E. and Ph.D. degrees from Kyoto University, Kyoto, Japan in 1988 and 2000, respectively. He joined NTT radio communications systems labs., Yokosuka, Japan, in 1988. In 1997, he was seconded to ATR adaptive communications research laboratories, Kyoto, Japan. From 2000 to 2002, he worked for NTT DoCoMo, Yokosuka, Japan. In 2002, he moved to DoCoMo communications laboratories Europe GmbH, Germany. From 2004 to 2011, he worked as an associate professor at Kyoto University. Since 2011, he is a full professor at graduate school of natural science and technology, Okayama University. From the beginning of his research carrier, he has been engaged in the research and development of digital mobile radio communications. In particular, he has considerable interests in channel equalization, array signal processing, Space time codes, spatial multiplexing, and multimode reception. He won the best paper award of the 19th international symposium on wireless personal multimedia communications in 2016. He received the Excellent Paper Award from the IEICE in 1995.

Kazuma Yamamoto received B.E. and M.E. degrees from Okayama University, Japan in 2018 and 2020, respectively. He joined with Shikoku Electric Power Company in 2020. His research interest is in signal detection and network coding in wireless communication systems.

Yafei Hou received the B.S. degree in electronic engineering from the Anhui University of Technology and Science, China, in 1999, the M.S. degree in computer science from Wuhan University, China, in 2002, and the Ph.D. degrees from Fudan University, China, and the Kochi University of Technology, Japan, in 2007. He was a Post-Doctoral Research Fellow with Ryukoku University, Japan, from 2007 to 2010. He was a Research Scientist with Wave Engineering Laboratories, ATR Institute International, Japan, from 2010 to 2014. From 2014 to 2016, he was an Assistant Professor with the Graduate School of Information Science, Nara Institute of Science and Technology, Japan. Since 2017, He has been an assistant professor at gradulate school of natural science and technology, Okayama University, Japan. His research interests are communication systems, wireless networks, and signal processing. He is a member of IEEE.